

Investigation of single spin asymmetries in π^+ electroproduction

K.A. Oganessyan^{ab*†}, N. Bianchi^a, E. De Sanctis^a, W.-D. Nowak^c

^aINFN-Laboratori Nazionali di Frascati, via Enrico Fermi 40, I-00044 Frascati, Italy

^bDESY, Notkestrasse 85, 22603 Hamburg, Germany

^cDESY Zeuthen, Platanenallee 6, D-15738 Zeuthen, Germany

The azimuthal single target-spin asymmetries for π^+ production in semi-inclusive deep inelastic scattering of leptons off longitudinally polarized protons are evaluated using two main approaches available in the literature. It is shown that the approximation where the twist-2 *transverse* quark spin distribution in the *longitudinally* polarized nucleon is small enough to be neglected leads to a consistent description of all existing asymmetries observed by the HERMES experiment.

PACS: 13.85.Ni, 13.87.Fh, 13.88.+e

1. Introduction

Semi-inclusive deep inelastic scattering (SIDIS) of leptons off a polarized nucleon

$$l + \vec{p} \rightarrow l' + h + X \quad (1)$$

is an important process to study the internal structure of the nucleon and its spin properties. In particular, measurements of azimuthal distributions of the detected hadron provide valuable information on hadron structure functions, quark-gluon correlations and parton fragmentation functions.

A significant target-spin asymmetry of the distributions in the azimuthal angle ϕ of the pion related to the lepton scattering plane for π^+ electroproduction in a *longitudinally* polarized hydrogen target has been recently observed by the HERMES collaboration [1,2]. At the same time the SMC collaboration has studied the azimuthal distributions of pions produced in deep inelastic scattering off *transversely* polarized protons and deuterons [3]. These results have been interpreted as the effects of *naive* “time-reversal-odd” (T-odd) fragmentation functions [4–8], arising from non-perturbative hadronic final-state interactions. They have initiated a number of phenomenological approaches to evaluate these asymmetries using different input distribution and fragmentation functions [9–15]. Actually, there are two main approaches in the literature which aim at explaining the experimental data:

*e-mail: kogan@hermes.desy.de

†On leave of absence from Yerevan Physics Institute, Alikhanian Br.2, AM-375036 Yerevan, Armenia

(i) The approximation where the twist-2 *transverse* quark spin distribution in the *longitudinally* polarized nucleon, $h_{1L}^{\perp(1)}(x)$, is considered small enough to be neglected [9–12]. This results in good agreement with the Bjorken- x behavior of the $\sin\phi$ and $\sin 2\phi$ asymmetries observed at HERMES. Note, that this does not require the twist-3 interaction-dependent part of the fragmentation function, $\tilde{H}(z)$, to be zero.

(ii) The approximation where the contribution of the interaction-dependent twist-3 term, $\tilde{h}_L(x)$, in the distribution function $h_L(x)$ is assumed to be negligible, but $\tilde{H}(z)$ is not constrained [10].

Another approximation, where only the twist-2 distribution and fragmentation functions are used, i.e. the interaction-dependent twist-3 parts of distribution and fragmentation functions are neglected, was proposed earlier [14,15]. For certain values of parameters this results in good agreement with the HERMES data [1]. However, it leads to the inconsistency that all T-odd fragmentation functions would be required to vanish [6,16]. Thus, in following we do not consider it anymore.

In this paper we provide an analysis in the framework of the two above given approximations to evaluate the single target-spin $\sin\phi$ and $\sin 2\phi$ asymmetries for π^+ production observed at HERMES [1,2] in semi-inclusive deep inelastic scattering of leptons off longitudinally polarized protons.

The paper is organized as follows: In Sec. 2 we define the single spin azimuthal asymmetries and the involved twist-2 and twist-3 distribution and fragmentation functions. In Sec. 3 we analyze the numerical results on the $\sin\phi$ and $\sin 2\phi$ asymmetries. In Sec. 4 we summarize the results.

2. Single spin asymmetries in $\gamma^* \vec{p} \rightarrow \pi X$

The kinematics of the process (1) is illustrated in Fig. 1: k_1 (k_2) is the 4-momentum of the incoming (outgoing) charged lepton, $Q^2 = -q^2$, where $q = k_1 - k_2$, is the 4-momentum of the virtual photon. P (P_h) is the momentum of the target (observed) hadron, $x = Q^2/2(Pq)$, $y = (Pq)/(Pk_1)$, $z = (PP_h)/(Pq)$, k_{1T} is the incoming lepton transverse momentum with respect to the virtual photon momentum direction, and ϕ is the azimuthal angle between P_{hT} and k_{1T} around the virtual photon direction. Note that the azimuthal angle of the transverse (with respect to the virtual photon) component of the target polarization, ϕ_S , is equal to 0 (π) for the target polarized parallel (anti-parallel) to the beam [17].

The $\sin\phi$ and $\sin 2\phi$ moments in the SIDIS cross-section can be related to the parton distribution and fragmentation functions involved in the parton level description of the underlying process [5,6]. These moments are defined as appropriately weighted integrals over P_{hT} (the transverse momentum of the observed hadron) of the cross section asymmetry:

$$\left\langle \frac{|P_{hT}|}{M_h} \sin\phi \right\rangle \equiv \frac{\int d^2 P_{hT} \frac{|P_{hT}|}{M_h} \sin\phi (d\sigma^+ - d\sigma^-)}{\int d^2 P_{hT} (d\sigma^+ + d\sigma^-)}, \quad (2)$$

$$\left\langle \frac{|P_{hT}|^2}{MM_h} \sin 2\phi \right\rangle \equiv \frac{\int d^2 P_{hT} \frac{|P_{hT}|^2}{MM_h} \sin 2\phi (d\sigma^+ - d\sigma^-)}{\int d^2 P_{hT} (d\sigma^+ + d\sigma^-)}. \quad (3)$$

Here $+(-)$ denotes the anti-parallel (parallel) longitudinal polarization of the target and M (M_h) is the mass of the target (final hadron).

The weighted single target-spin asymmetries defined above are related to the ones measured by HERMES [1] through the following relations:

$$A_{UL}^{\sin\phi} \approx \frac{2M_h}{\langle P_{hT} \rangle} \left\langle \frac{|P_{hT}|}{M_h} \sin \phi_h \right\rangle, \quad (4)$$

$$A_{UL}^{\sin 2\phi} \approx \frac{2MM_h}{\langle P_{hT}^2 \rangle} \left\langle \frac{|P_{hT}^2|}{MM_h} \sin 2\phi_h \right\rangle, \quad (5)$$

where the subscripts U and L indicate unpolarized beam and longitudinally polarized target, respectively.

These asymmetries are given by [5,6,17] ³

$$\left\langle \frac{|P_{hT}|}{M_h} \sin \phi_h \right\rangle = \frac{1}{I_0} [I_{1L} + I_{1T}], \quad (6)$$

$$\left\langle \frac{|P_{hT}|^2}{MM_h} \sin 2\phi_h \right\rangle = \frac{8}{I_0} S_L(1-y) h_{1L}^{\perp(1)}(x) z^2 H_1^{\perp(1)}(z), \quad (7)$$

where

$$I_0 = (1 + (1+y)^2) f_1(x) D_1(z), \quad (8)$$

$$\begin{aligned} I_{1L} &= 4S_L \frac{M}{Q} (2-y) \sqrt{1-y} [-2h_{1L}^{\perp(1)}(x) z H_1^{\perp(1)}(z) \\ &+ x \tilde{h}_L(x) z H_1^{\perp(1)}(z) - h_{1L}^{\perp(1)}(x) \tilde{H}(z)], \end{aligned} \quad (9)$$

$$I_{1T} = 2S_{Tx} (1-y) h_1(x) z H_1^{\perp(1)}(z). \quad (10)$$

Here the components of the longitudinal and transverse target polarization in the virtual photon frame are denoted by S_L and S_{Tx} , respectively. Twist-2 distribution and fragmentation functions have a subscript ‘1’: $f_1(x)$ and $D_1(z)$ are the usual unpolarized distribution and fragmentation functions, while $h_{1L}^{\perp(1)}(x)$ and $h_1(x)$ describe the quark transverse spin distribution in longitudinally and transversely polarized nucleons, respectively. The interaction-dependent part of the twist-3 distribution function in the longitudinally polarized nucleon, $h_L(x)$ [18], is denoted by $\tilde{h}_L(x)$ [19,20].

For approach (i), where the twist-2 *transverse* quark spin distribution in the *longitudinally* polarized nucleon, $h_{1L}^{\perp(1)}(x)$, is set to zero, it follows:

$$h_L(x) = \tilde{h}_L(x) = h_1(x). \quad (11)$$

In approach (ii) the interaction-dependent twist-3 part, $\tilde{h}_L(x)$, of the twist-3 distribution function, $h_L(x)$, is set to zero and hence [19,20]:

$$h_{1L}^{\perp(1)}(x) = -x^2 \int_x^1 dy \frac{h_1(x)}{y^2}. \quad (12)$$

³We omit the current quark mass dependent terms.

It is worth noting here that calculations performed in the instanton model of Quantum Chromodynamics [21] indicate the parametric smallness of the twist-3 contribution to the polarized structure function, while in the bag model this twist-3 contribution is comparable to the twist-2 contribution at small Q^2 [19,22].

The spin-dependent fragmentation function $H_1^{\perp(1)}(z)$, describing transversely polarized quark fragmentation [4], correlates the transverse spin of a quark with a preferred transverse direction for the production of the pion. The fragmentation function $\tilde{H}(z)$ is the interaction-dependent part of the twist-3 fragmentation function, $H(z)$, [6] and is directly connected to $H_1^{\perp(1)}(z)$:

$$\tilde{H}(z) = z \frac{d}{dz} (z H_1^{\perp(1)}(z)). \quad (13)$$

The distribution and fragmentation functions with superscript (1) denote p_T^2 , k_T^2 - moments, where p_T , k_T are the intrinsic transverse momenta of the initial and final quark, respectively.

3. Numerical results

For the numerical calculations in this work the non-relativistic approximation $h_1(x) = g_1(x)$ is used as a lower limit ⁴, and $h_1(x) = (f_1(x) + g_1(x))/2$ as an upper limit [27]. For the sake of simplicity, Q^2 -independent parameterizations were chosen for the distribution functions $f_1(x)$ and $g_1(x)$ [28].

To obtain the T-odd fragmentation function $H_1^{\perp(1)}(z)$, the Collins ansatz [4] for the analyzing power of transversely polarized quark fragmentation was adopted:

$$A_C(z, k_T) \equiv \frac{|k_T|}{M_h} \frac{H_1^{\perp}(z, k_T^2)}{D_1(z, k_T^2)} = \eta \frac{M_C |k_T|}{M_C^2 + k_T^2}, \quad (14)$$

where η is taken as a constant, although, in principle it could be z dependent.

For the distribution of the final parton intrinsic transverse momentum, k_T , in the unpolarized fragmentation function $D_1(z, k_T^2)$, a Gaussian parameterization was used [29] with $\langle z^2 k_T^2 \rangle = b^2$ (in the numerical calculations $b = 0.36$ GeV was taken [30]). For $D_1^{\pi^+}(z)$, the parameterization from Ref. [31] was adopted. In Eq.(14) M_C is a typical hadronic mass whose value ranges from $2m_\pi$ to M_p .

It is important to point out here that the T-odd fragmentation function calculated with the Collins ansatz (Eq.(14)) at a reasonable value of the parameter M_C ($M_C = 2m_\pi$) with $\eta = 1.0$, turns out to be in very good agreement with the parameterization [10,32] that was based on a fit of $pp^\uparrow \rightarrow \pi X$ experimental data [33]. In our calculations a good agreement with HERMES results was achieved at that value of M_C , with $\eta = 0.8$. This value of η may indicate possible contributions of other mechanisms [34,35] in $pp^\uparrow \rightarrow \pi X$.

In Fig. 2, the asymmetry $A_{UL}^{\sin\phi}(x)$ of Eq.(4) for π^+ production on a proton target evaluated within the two approaches described in the Sec. 1, is presented as a function of

⁴In the non-relativistic quark model $h_1(x, \mu_0^2) = g_1(x, \mu_0^2)$. Several models suggest that $h_1(x)$ is close to g_1 [19,23,24]. The evolution properties of h_1 and g_1 , however, are very different [25]. At the Q^2 values of the HERMES measurement the assumption $h_1 = g_1$ is fulfilled at large, i.e. valence-like, x values, while large differences occur at lower x [26].

Bjorken- x and compared to HERMES data [1], which correspond to $1 \text{ GeV}^2 \leq Q^2 \leq 15 \text{ GeV}^2$, $4.5 \text{ GeV} \leq E_\pi \leq 13.5 \text{ GeV}$, $0.02 \leq x \leq 0.4$, $0.2 \leq z \leq 0.7$, and $0.2 \leq y \leq 0.8$.

The curves have been calculated by integrating over the HERMES kinematic range taking $\langle P_{hT} \rangle = 0.365 \text{ GeV}$ and $\langle P_{hT}^2 \rangle = 0.165 \text{ GeV}^2$ as input. The latter values are obtained in this kinematic region assuming a Gaussian parameterization of the distribution and fragmentation functions with $\langle p_T^2 \rangle = (0.44)^2 \text{ GeV}^2$ [30].

The results obtained within the approaches (i) and (ii) are denoted by pairs of full and dashed lines, respectively. For each approach two curves are presented according to the upper and lower limits chosen for $h_1(x)$.

From Fig. 2 it can be concluded that there is good agreement between results of the approach (i) and the HERMES data. The results of approach (ii) appear too low.

Note that the ‘kinematic’ contribution to $A_{UL}^{\sin\phi}(x)$, coming from the transverse component of the target polarization with respect to the virtual photon direction and given by I_{1T} (Eq.(10)), is about (45 – 50)% in approach (ii). In approach (i), where the twist-3 part of the fragmentation functions does not contribute (because of $h_{1L}^{\perp(1)}(x) \approx 0$) [9–12], it amounts to 25%.

The z dependence of the asymmetry $A_{UL}^{\sin\phi}$ is shown in Fig. 3 and compared with HERMES preliminary data [2], which here extend up to $z = 1$. In approach (i) the $\sin\phi$ asymmetry increases with z and is in good agreement with data up to $z = 0.8$. The sharp decrease of data for higher z values reflects the transition from the semi-inclusive to the exclusive regime which requires a different investigation. In this respect our calculations are limited to $z \leq 0.9$. In approach (ii) the behavior of the asymmetry is quite different from that in approach (i) and fails to describe the experimental data already above $z \approx 0.5$.

Finally, in Fig. 4 the asymmetry $A_{UL}^{\sin 2\phi}$ of Eq.(5) is presented for π^+ production on a proton target as a function of Bjorken- x and compared to HERMES data [1]. Approach (ii), where $h_{1L}^{\perp(1)}(x) = 0$, leads directly to $A_{UL}^{\sin 2\phi} = 0$ in better agreement with the data. The curves from approach (ii) are also compatible with the data, taking into account their total accuracy. Clearly, more accurate data will better constrain the phenomenological predictions. It is worth mentioning that by changing the parameters of the input functions it is possible to increase the magnitude of the $|A_{UL}^{\sin\phi}|$ asymmetry calculated in the approach (ii). However, this also modifies the z -dependence leading to a stronger disagreement with the data, and also increases the magnitude of the calculated asymmetry $|A_{UL}^{\sin 2\phi}|$ deteriorating the compatibility with the data.

In addition we note that approach (i) well describes the P_{hT} dependence of $A_{UL}^{\sin\phi}$ observed at HERMES [36], too.

4. Conclusions

We have evaluated the $A_{UL}^{\sin\phi}$ and $A_{UL}^{\sin 2\phi}$ single-spin asymmetries for semi-inclusive π^+ production in semi-inclusive deep inelastic scattering of leptons off longitudinally polarized protons using the two main approaches available in the literature. The results have been compared to the recent HERMES data. The approximation where the twist-2 *transverse* quark spin distribution in the *longitudinally* polarized nucleon, $h_{1L}^{\perp(1)}(x)$, is neglected, gives a consistent description of both $A_{UL}^{\sin\phi}(x)$ and $A_{UL}^{\sin 2\phi}(x)$ and describes well the z -dependence

of $A_{UL}^{\sin\phi}$.

5. Acknowledgments

We thank Daniel Boer, Bob Jaffe, Aram Kotzinian and Piet Mulders for interesting discussions. The work of K.A.O. was in part supported by INTAS contributions (contract numbers 93-1827 and 96-287) from the European Union.

REFERENCES

1. H. Avakian, for the HERMES Collaboration, Nucl. Phys. (Proc. Suppl.) **B79** (1999) 523; HERMES Collaboration, A. Airapetian, et.al, Phys. Rev. Lett. **84** (2000) 4047.
2. D. Hasch, for the HERMES collaboration, 35th Rencontres de Moriond: QCD and Hadronic Interactions, Les Arcs, France, March 18 - 25, 2000.
3. A. Bravar, Nucl. Phys. (Proc. Suppl.) **B79** (1999) 520.
4. J. Collins, Nucl. Phys. **B396** (1993) 161.
5. A. Kotzinian, Nucl. Phys. **B441** (1995) 234.
6. P.J. Mulders and R.D. Tangerman, Nucl Phys. **B461** (1996) 197.
7. X. Artru, J. Czyzewski and H. Yabuki, Z. Phys **C73**, (1997) 527.
8. R. Jaffe, X. Ji and J. Tang, Phys. Rev. Lett. **80** (1998) 1166.
9. D. Boer, hep-ph/9912311.
10. M. Boglione and P.J. Mulders, Phys. Lett. **B478** (2000) 114.
11. A.V. Efremov, hep-ph/0001214.
12. E. De Sanctis, W.-D. Nowak, and K.A. Oganessyan, Phys. Lett. **B483** (2000) 69.
13. M. Anselmino and F. Murgia, hep-ph/0002120.
14. A.M. Kotzinian, K.A. Oganessyan, A.R. Avakian, and E. De Sanctis, Nucl. Phys. **A666-667** (2000) 290.
15. A.V. Efremov, M. Polyakov, K. Goeke, and D. Urbano, Phys. Lett. **B478** (2000) 94.
16. A. Schaefer and O.V. Teryaev, Phys. Rev. **D61** (2000) 077903.
17. K.A. Oganessyan, A.R. Avakian, N. Bianchi, and A.M. Kotzinian, hep-ph/9808368; Proceedings of the workshop Baryons'98, Bonn, Sept. 22-26, 1998.
18. R. Jaffe, and X. Ji, Phys. Rev. Lett, **67** (1991) 552.
19. R. Jaffe, and X. Ji, Nucl. Phys. **B375** (1992) 527.
20. R.D. Tangerman, and P.J. Mulders, NIKHEF-94-P7, hep-ph/9408305.
21. B. Dressler, and M.V. Polyakov, Phys.Rev. **D61** (2000) 097501.
22. Y. Kanazawa, and Y. Koike, Phys.Lett. **B403** (1997) 357.
23. P.V. Pobylitsa and M.V. Polyakov, Phys. Lett. **B389** (1996) 350.
24. V. Barone, T. Calarco and A. Drago, Phys. Lett. **B390** (1997) 287.
25. S. Scopetta, and V. Vento, Phys.Lett. **B424** (1998) 25.
26. V.A. Korotkov, W.-D. Nowak, and K.A. Oganessyan, hep-ph/0002268; DESY 99-176.
27. J. Soffer, Phys. Rev. Lett. **74** (1995) 1292.
28. S. Brodsky, M. Burkardt, and I. Schmidt, Nucl. Phys. **B441** (1995) 197.
29. A.M. Kotzinian, and P.J. Mulders, Phys. Lett. **B406** (1997) 373.
30. T. Sjostrand, Comp. Phys. Commun. **82** (1994) 74; CERN-TH.7112/93; hep-ph/9508391.
31. E. Reya, Phys. Rep. **69** (1981) 195.

32. M. Boglione, and E. Leader, hep-ph/9911207. (1999) 054007.
33. D.L. Adams, et.al., Phys. Lett. **B261** (1991) 201; Phys. Lett. **B264** (1991) 462.
34. A.V. Efremov, O.V. Teryaev, Phys. Lett. **B150** (1985) 383.
35. J. Qiu, G. Sterman, Phys. Rev. Lett. **67** (1991) 2264; Nucl. Phys. **B378** (1992) 52.
36. K.A. Oganessyan, N. Bianchi, E. De Sanctis, and W.-D. Nowak, hep-ph/0010063; Proceedings of the Euroconference QCD'00, 6-13 July, 2000, Montpellier.

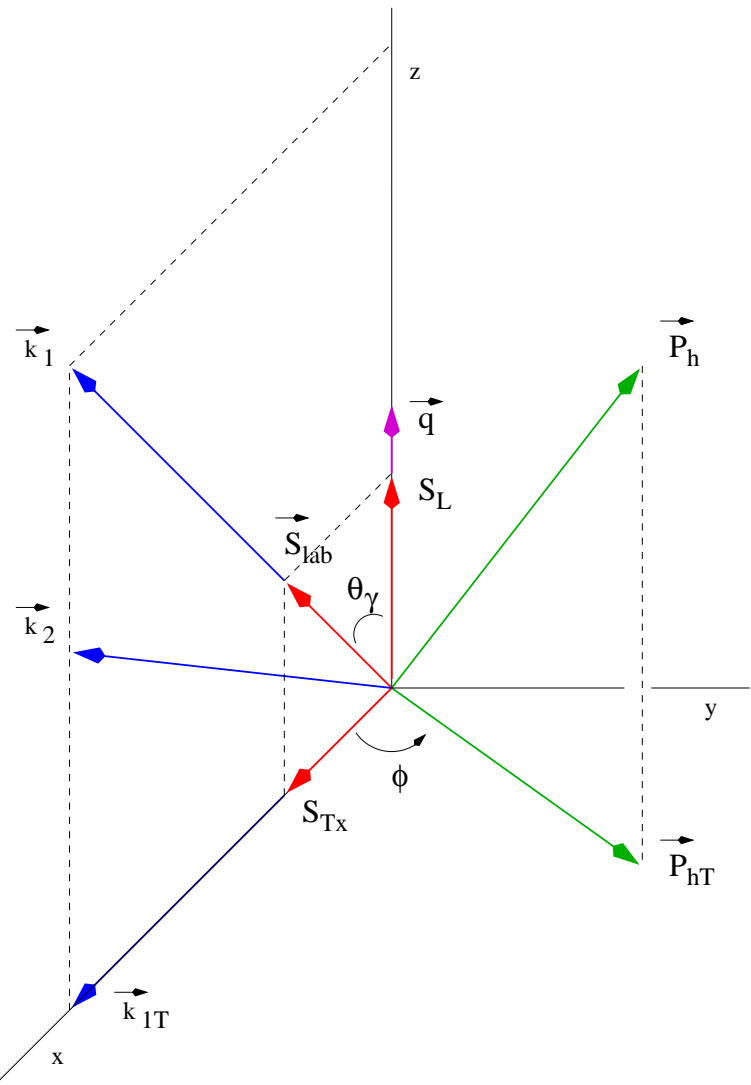


Figure 1. The kinematics of the process (1).

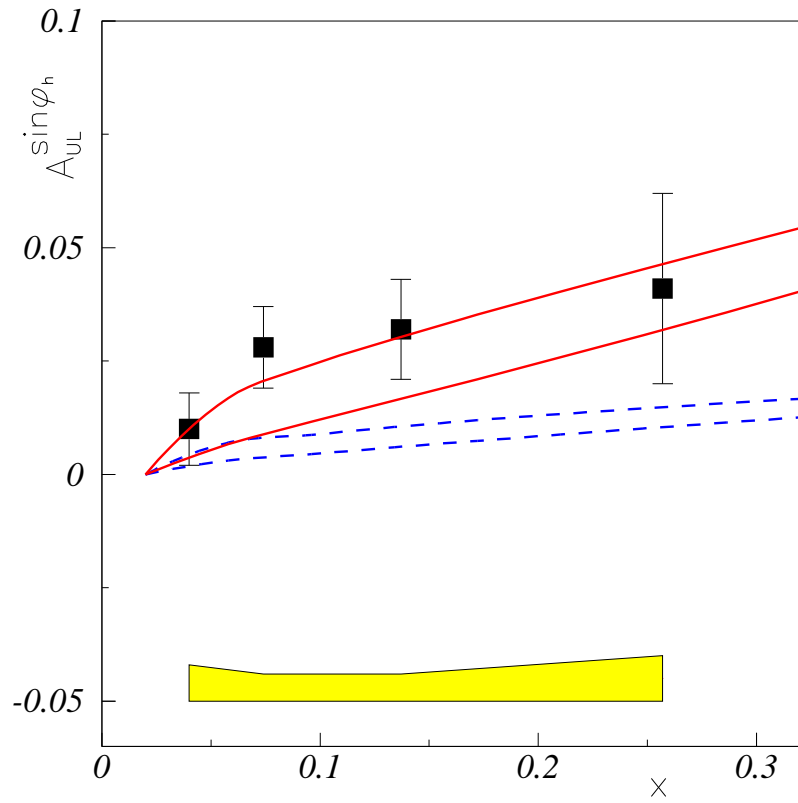


Figure 2. The single target-spin asymmetry $A_{UL}^{\sin\phi}$ for π^+ production as a function of Bjorken- x , evaluated using $M_C = 2m_\pi$ and $\eta = 0.8$ in Eq.(14). The results obtained within approaches (i) and (ii) are denoted by pairs of full and dashed lines, respectively. For each approach two curves are presented corresponding to $h_1 = g_1$ (lower curve) and $h_1 = (f_1 + g_1)/2$ (upper curve). HERMES data are from Ref. [1].

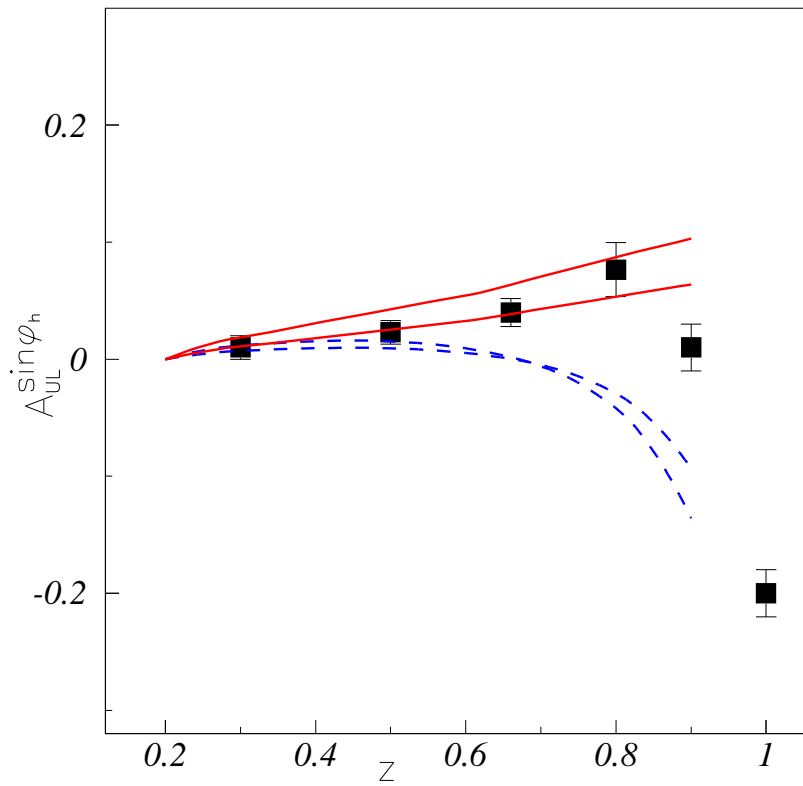


Figure 3. The single target-spin asymmetry $A_{UL}^{\sin\phi}$ for π^+ production as a function of z evaluated using the same parameters as in Fig. 2. The curves have the same notations as in the Fig. 2. HERMES preliminary data not corrected for smearing (the error bars correspond to the statistical uncertainties only), are taken from Ref. [2].

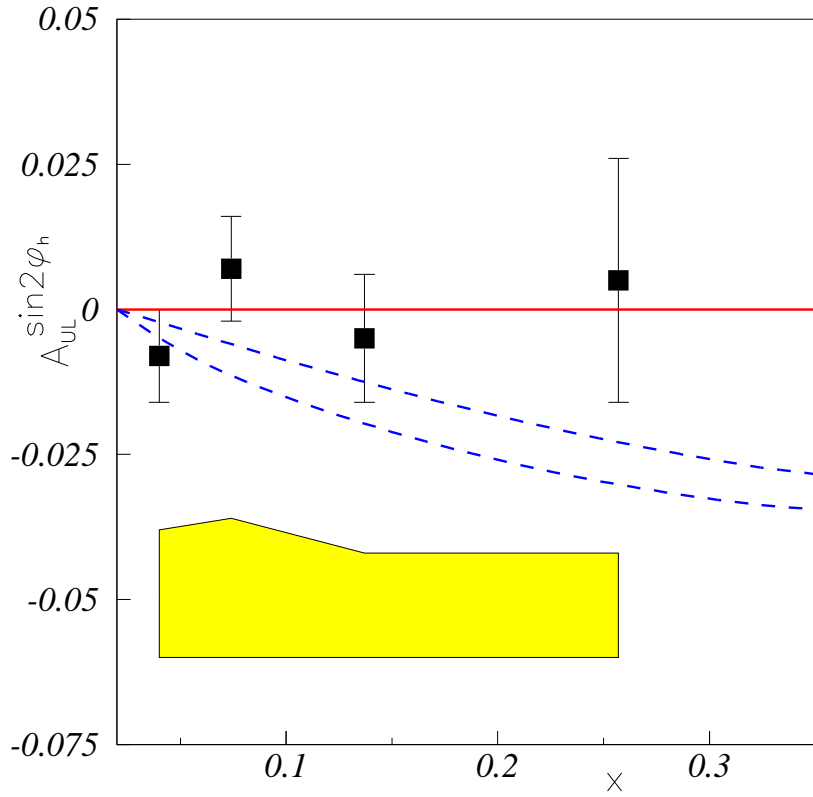


Figure 4. The single target-spin asymmetry $A_{UL}^{\sin 2\phi}$ for π^+ production as a function of Bjorken x , evaluated using the same parameters as in Fig. 2. The curves have the same notations as in the Fig. 2; the line at $A_{UL}^{\sin 2\phi} = 0$ corresponds to the result of approach (i). Data are from Ref. [1].